PNAS RESEARCH ARTICLE | PHYSICS ECOLOGY

Delay effects on the stability of large ecosystems

Emanuele Pigani[a,b,1], Damiano Sgarbossa[c], Samir Suweis[a,d], Amos Maritan[a,d], and Sandro Azaele[a,d]

Edited by Pablo Marquet, Pontificia Universidad Catolica de Chile, Santiago, Chile; received July 6, 2022; accepted September 26, 2022

The common intuition among the ecologists of the midtwentieth century was that large ecosystems should be more stable than those with a smaller number of species. This view was challenged by Robert May, who found a stability bound for randomly assembled ecosystems; they become unstable for a sufficiently large number of species. In the present work, we show that May's bound greatly changes when the past population densities of a species affect its own current density. This is a common feature in real systems, where the effects of species' interactions may appear after a time lag rather than instantaneously. The local stability of these models with self-interaction is described by bounds, which we characterize in the parameter space. We find a critical delay curve that separates the region of stability from that of instability, and correspondingly, we identify a critical frequency curve that provides the characteristic frequencies of a system at the instability threshold. Finally, we calculate analytically the distributions of eigenvalues that generalize Wigner's as well as Girko's laws. Interestingly, we find that, for sufficiently large delays, the eigenvalues of a randomly coupled system are complex even when the interactions are symmetric.

time delay systems | random matrix theory | linear stability analysis

Significance

Understanding how communities emerge from a large number of interacting entities is a long-standing question in several fields. In ecosystems with randomly coupled species, a delayed dynamics seemed to play a minor role in characterizing the stability close to equilibrium. Here, we study the effects on large ecosystems of species' interactions that are random as well as delayed. We find that near equilibrium, delayed self-interactions greatly modify the eigenspectrum distribution as predicted by Wigner's as well as Girko's laws. We analytically calculate the ensued generalized laws and identify the geometric profile of the eigenvalues in the complex plane.

The study of large communities of interacting entities has been the focus of disparate fields of research in the last decades (1–5) and has witnessed important strides of progress. One of the endeavors is to discover what the minimal ingredients are that beget persistent coexistence (6, 7). What are the key features of the interactions that lead communities, such as bacterial colonies (8, 9) or ecological systems (10, 11), to become diverse and stable assemblies of entities?

A thread of research dates back to May's work (12) and has recently gained momentum. It is motivated by the lack of knowledge about species' interactions in large communities and relies on the study of disordered Lotka–Volterra or replicator equations (13–18). Global analysis of fairly general nonlinear systems with random couplings has pointed out the existence of a sharp transition between a phase portrait with a single stable equilibrium and another one with exponentially many equilibria, which are unstable on average (19, 20). Surprisingly, the transition has a structure that is similar to the local instability threshold found by May (12) in his seminal paper. Other studies have highlighted that disordered ecosystems are marginally stable as a large fraction of species grows strong and heterogeneous interactions (21, 22). Thus, strong random couplings drive large systems close to May's bound, where they are susceptible to tiny perturbations.

Chaotic coexistence has instead challenged equilibrium stability and ecological neutrality as a possible mechanism promoting extensive diversity. Albeit chaos per se can shatter diversity by triggering a cascade of extinctions (23), a simple spatial structure can nevertheless sustain a phase of spatiotemporal chaos, which robustly maintains diversity (23, 24).

Spatial degrees of freedom may introduce effective delayed dynamics in mean field models (25). Let us consider, for instance, the simple case of a species whose population moves on a one-dimensional lattice with a logistic dynamics. When taking the mean field approximation of the model, the common approach suggests to remove spatial diffusion and consider the simpler logistic evolution. However, one could alternatively coarse grain the spatial degrees of freedom (25) and find an effective dynamics, in which spatial diffusion is eventually removed. This latter approach is not equivalent to the former and has the benefit to include spatial effects into mean field models. In the more general case of randomly interacting species, this mean field approximation has the advantage to include spatial effects in May's formulation of the problem. In *SI Appendix*, we show that a coarse graining of the spatial degrees of freedom can generate a delayed dynamics, which includes delayed self-interactions. These latter have important consequences for May's bound as we show in the following sections. Indeed, an arbitrary delay that does not affect species' own density (i.e., in the absence of delayed self-interaction) would not modify May's conclusions, as it has been clarified in ref. 26. However, we argue that the presence of delayed self-interactions is by far the most common situation in real ecosystems.

Author affiliations: [a]Dipartimento di Fisica "G. Galilei," Università di Padova, 35131 Padova, Italy; [b]Integrative Marine Ecology Department, Stazione Zoologica Anton Dohrn, 80121 Naples, Italy; [c]Institute of Bioengineering, School of Life Sciences, Ecole Polytechnique Fédérale de Lausanne, 1015 Lausanne, Switzerland; and [d]Istituto Nazionale di Fisica Nucleare, 35131, Padova, Italy

Author contributions: S.A. and A.M. designed research; E.P., D.S., S.S., A.M., and S.A. performed research; and E.P., D.S., S.S., A.M., and S.A. wrote the paper.

The authors declare no competing interest.

This article is a PNAS Direct Submission.

[1]To whom correspondence may be addressed. Email: emanuele.pigani.1@unipd.it.

This article contains supporting information online at https://www.pnas.org/lookup/suppl/doi:10.1073/pnas.2211449119/-/DCSupplemental.

Published November 2, 2022.

The empirical evidence that the effects of species' interactions usually appear after a time lag, rather than instantaneously (27–29), suggests that delay could have important implications for coexistence and diversity. More specifically, considering that it can elicit chaotic features even in simple logistic models (30, 31), delayed dynamics could potentially clarify how interacting populations generate chaotic coexistence.

In the present work, we apply the theory of random matrices to study the effects of delayed interactions on large systems near stationarity. In the spirit of May's approach, we focus on the linear and stationary regime of interacting population dynamics, in which the couplings are random and delayed. May (12) found that, with no delay, there exists a critical threshold above which the stationary state is almost surely unstable; if the interactions are too strong or there are too many species, a system becomes unstable. Some refinements of May's paper (12) have weakened the range of validity of his result (32). Here, however, we restrict ourselves to systems where May's critical threshold is correct.

We generalize his result, identify analytically stability criteria, and calculate the geometric profile of the eigenspectrum, which no longer follows the circular law. We first show the existence of a critical delay curve, which depends on the number of interacting species and above which the system is unstable. Correspondingly, there is also a critical frequency curve that depends on the system size and describes the oscillations of the population densities at the instability threshold. Finally, we calculate analytically the distributions of the eigenvalues, which generalize Wigner's semicircle as well as Girko's circle laws. For sufficiently large delays, we find complex eigenvalues even when the interactions are symmetric and multimodal distributions for the real and imaginary parts of the eigenvalues for asymmetric random interactions.

Results

Discrete Delay. We model an ecological community of S different interacting species with a (continuous-time) dynamical system that governs the evolution of the population densities. The growth rate of a population is ruled by the densities at time t as well as those at the previous time $t-\tau$, with τ being a positive time delay. Hence, the starting equation is $\dot{z}_i(t) = f_i(z(t), z(t-\tau))$ for $i = 1, \dots, S$, where $z_i(t)$ is the population density of species i at time t and f_i is a smooth function of its arguments. If we now assume that the dynamics admits a strictly positive equilibrium point and we restrict our scope to studying its local asymptotic stability, we end up with a linear system of delayed differential equations for the deviation of the density of species i from its equilibrium [i.e., $x_i(t) = z_i(t) - z_i^*$], which has the form

$$\dot{x}_i(t) = \sum_{j=1}^{S} A_{ij} x_j(t) + \sum_{j=1}^{S} B_{ij} x_j(t-\tau), \qquad [1]$$

where $A_{ij} = \frac{\partial f_i}{\partial z_j(t)}\big|_{z^\star}$ and $B_{ij} = \frac{\partial f_i}{\partial z_j(t-\tau)}\big|_{z^\star}$ are the community matrices that provide the current and delayed coupling strengths between species i and j (33). For the sake of simplicity, we will assume that the two matrices commute, so that the eigenmode equation for the dynamics is decoupled. Hence, by making the ansatz for the eigenvectors $u_i \propto e^{\lambda_i t}$, the transcendental equation satisfied by the eigenvalues λ_i of the system is

$$\lambda_i = a_i + b_i e^{-\lambda_i \tau}, \qquad [2]$$

where a_i and b_i are the (complex) eigenvalues of A and B, respectively. Indeed, the local asymptotic stability of equilibrium densities ensues from the condition $\mathrm{Re}[\lambda_i] < 0$ for any i (34). The solution of Eq. **2** for λ_i as a function of the delay τ and the eigenvalues of A and B is given by

$$\lambda_i = a_i + \frac{\mathcal{W}\left(b_i \tau e^{-a_i \tau}\right)}{\tau}, \qquad [3]$$

where $\mathcal{W}(\cdot)$ is the Lambert $\mathcal{W}$ function (35), which is a multivalued function and is implicitly defined through the identity $\mathcal{W}(z) e^{\mathcal{W}(z)} = z$.

We consider here the simple situation where $A = -d_A \mathbb{1}$ with $d_A \geq 0$, which guarantees the commutativity of matrices. This allows us to study the effect of the delay more closely while ensuring stability for a sufficiently small community matrix delay. From the ecological standpoint, we focus on systems in which self-interaction has two components; current intraspecies couplings are always stabilizing, whereas there exist intraspecies interactions that occurred in the past and have an effect on the current growth rate of the population densities. We then suppose B to be a random matrix with a constant diagonal entry $-d_B \leq 0$ and off-diagonal elements normally distributed with zero mean, SD σ, and connectance C, where C does not depend on S, and it is the probability that an interaction occurs between a pair of species. Under this hypothesis, the eigenspectrum of B follows the circular law (12); namely, it belongs to a circle $\mathcal{C}$ centered at $(-d_B; 0)$ with radius $r_B \equiv \sigma\sqrt{SC}$ in the large size S limit. As anticipated, d_A and d_B are in general different since a variety of ecological effects may induce different current and delayed interactions. Furthermore, even though in the following, we assume the diagonal elements A_{ii} and B_{ii} to be constant, the results are robust for a larger class of matrices: that is, for random delayed intraspecies interactions inasmuch as their fluctuations are comparable with the ones of the interspecies interactions. In addition, in *SI Appendix*, we also consider a case of noncommuting matrices. In particular, we allow the undelayed interaction matrix to also account for interspecies interactions, which are modeled as a small perturbation of the constant intraspecies interaction matrix $-d_A \mathbb{1}$. By means of perturbation theory, we derive an analytical expansion at the first order for the system eigenspectrum. Furthermore, in *SI Appendix*, we numerically show that the system eigenspectrum weakly changes when we also allow the current intraspecies interactions A_{ii} to be normally distributed as long as their SDs do not exceed σ.

For a given set of parameters d_A, d_B, and r_B, from Eq. **2** one can derive the equation of the profile of the eigenvalues λ_i (*SI Appendix*) as a function of τ:

$$d_B^2 + 2 d_B e^{\tau\Lambda}\left[(d_A + \Lambda)\cos(\tau\omega) - \omega \sin(\tau\omega)\right] + \\ + e^{2\tau\Lambda}\left[(d_A + \Lambda)^2 + \omega^2\right] = r_B^2, \qquad [4]$$

where $\Lambda \equiv \mathrm{Re}[\lambda]$ and $\omega \equiv \mathrm{Im}[\lambda]$. This is plotted in Fig. 1, *Inset*. Conditions for Λ, ω, and τ have already been obtained from Eq. **2** (26, 33); here, Eq. **4** is instrumental to our main findings and for showing how $d_B > 0$ changes the profile of the eigenspectrum. We now focus only on the rightmost part since local stability depends only on the eigenvalues with the largest real part. However, it is not difficult to obtain the entire profile of the eigenspectrum through the branches of the Lambert function.

As expected, if $\tau = 0$, Eq. **4** reduces to the one of a circle with a radius r_B and the center at $(-d_A - d_B, 0)$. Thus, we recover May's condition $r_B < d_A + d_B \equiv r_B^\star$. When τ is larger than zero, two wings bulge, with the tips pointing toward the imaginary axis. If we fix the system size so that it is stable for $\tau = 0$, as in Fig. 1, *Inset*, we notice that an increasing delay tends

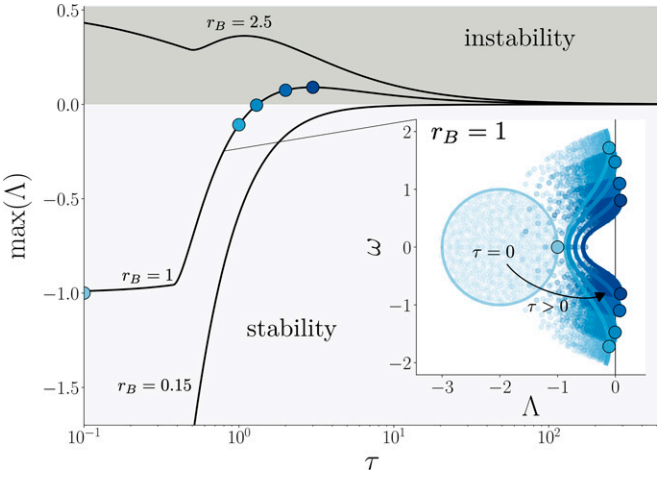

Fig. 1. Maximum of the real part Λ of the eigenspectrum (Eq. **2**) as a function of the discrete delay τ when $A = -d_A\mathbb{1}$ and B is a random matrix for three representative values of $r_B = \sigma\sqrt{SC}$ (black solid lines). When $r_B = 0.15$, the system is always stable since $\max(\Lambda) < 0$ for any τ. Conversely, when $r_B = 2.5$, the system is always unstable since $\max(\Lambda) > 0$ for any τ. When $r_B = 1$, there is a critical delay $\tau^\star$ for which $\max(\Lambda) = 0$ (•). The real part Λ vs. the imaginary part ω of the eigenvalues is shown in *Inset*, where the rightmost profiles of the eigenspectrum (blue solid lines) are plotted for increasing values of τ (according to the direction of the arrow) when $r_B = 1$. We recognize the circular law (12) for $\tau = 0$, while for $\tau > 0$, we observe wing-like shapes, which lead to instability as soon as they cross the imaginary axis. The solid lines depict solutions of Eq. **4** (for different delays), and the color-coded points represent the point with the highest real part of a given profile. Here, $d_A = 1.1$ and $d_B = 0.9$ in both the main panel and *Inset*. In *Inset*, $C = 0.1$, $\sigma = 0.1$, and $S = 1{,}000$, whereas $\tau = 0, 1, 1.3, 2$, and 3.

to destabilize the system. In particular, as τ increases, the wings cross the imaginary axis, and the system becomes unstable. On the other hand, if a system is unstable for $\tau = 0$ (i.e., if $r_B > r_B^\star$), the delay cannot stabilize the system as illustrated in Fig. 1.

For studying this instability, it is convenient to define a critical delay $\tau^\star$ as the minimum value of τ, above which the system becomes unstable [i.e., above which $\max(\Lambda) > 0$], with all the other parameters being fixed. As exemplified in Fig. 1, there are three possible scenarios, which depend on the parameters. If $r_B \geq r_B^\star$, the system is already unstable for $\tau = 0$, and hence, we set $\tau^\star = 0$. If instead, the system is stable for any arbitrary τ, then $\tau^\star = \infty$. The intermediate case occurs when the largest eigenvalue crosses the imaginary axis for a finite critical delay (i.e., $0 < \tau^\star < \infty$).

Remarkably, it is possible to obtain from Eq. **4** two independent conditions for determining $\tau^\star$ and the corresponding critical frequency $\omega^\star$, at which the transition from the stable to the unstable regime occurs. As shown in *Materials and Methods*, they read

$$d_B^2 + d_A^2 + \omega^{\star 2} + 2d_B\left[d_A\cos\left(\omega^\star\tau^\star\right) - \omega^\star\sin\left(\omega^\star\tau^\star\right)\right] = r_B^2, \quad [5]$$

$$\left(1 + d_A\tau^\star\right)d_B\sin\left(\omega^\star\tau^\star\right) + d_B\omega^\star\tau^\star\cos\left(\omega^\star\tau^\star\right) = \omega^\star. \quad [6]$$

Interestingly, when $d_B = 0$, these two equations are satisfied if and only if $\omega = 0$ and $r_B = d_A$. This means that the stability does not depend on τ, as already found in ref. 26; the system is stable for any τ when $r_B < d_A$ ($\tau^\star = \infty$), whereas it becomes unstable as soon as $r_B \geq d_A$ ($\tau^\star = 0$), regardless of τ. In this case, May's bound is not affected by the delay, and the circular law is still valid. This result as well as conditions for Λ, ω, and τ for $d_B = 0$ can be obtained directly from Eq. **2** (26, 33). However, when d_B is strictly positive, $\tau^\star$ becomes a nontrivial function of d_B, d_A, and r_B, as shown in Fig. 2. Therein, we have fixed d_A and d_B, and we have investigated the dependence of $\tau^\star$ and $\omega^\star$ on the system size through r_B. First of all, we observe the presence of three regimes for $\tau^\star$: $\tau^\star = \infty$ when $0 \leq r_B \leq \max\{0, d_A - d_B\}$, $0 < \tau^\star(r_B) < \infty$ when $\max\{0, d_A - d_B\} < r_B < d_A + d_B$, and $\tau^\star = 0$ when $r_B \geq d_A + d_B$. Remarkably, $\tau^\star(r_B)$ diverges as r_B approaches $d_A - d_B \geq 0$, whereas it has a finite jump $\tau_0^\star$ when r_B approaches $d_A + d_B$. As a consequence, May's stability condition $r_B < r_B^\star = d_A + d_B$ is still valid as long as $\tau \leq \tau_0^\star$. On the other hand, when $\tau > \tau_0^\star$, a more restrictive condition for the stability holds (i.e., the system becomes unstable for smaller S). Although Eqs. **5** and **6** cannot be explicitly solved, for $d_A > 0$ it is still possible to find the value of the finite jump $\tau_0^\star$, which reads

$$\tau_0^\star\left(d_A, d_B\right) = \frac{\sqrt{1 + d_A/d_B} - 1}{d_A} \quad [7]$$

and becomes simply $\tau_0^\star = 1/(2d_B)$ in the interesting case of a pure delayed dynamics (i.e., when $d_A = 0$). On the other hand, when $d_B \to 0^+$, $\tau_0^\star$ diverges, and again, we recover that in this case, May's condition is valid regardless of τ. Furthermore, it is also possible to find the asymptotic behavior for $\tau^\star$ and $\omega^\star$ as r_B is close to $\max\{0, d_A - d_B\}$ or $d_A + d_B$, and it is nonanalytic at both boundaries. In this latter case, their series expansion at both boundaries has been exploited for getting both local and global approximated solutions for Eqs. **5** and **6**, as demonstrated in *SI Appendix*.

Distributed Delay. When including a distributed delay in the dynamics, Eq. **1** has to be replaced by

$$\dot{x}_i(t) = \sum_{j=1}^{S} A_{ij}x_j(t) + \sum_{j=1}^{S} B_{ij}\int_0^\infty \mathrm{d}\tau f(\tau)x_j(t-\tau), \quad [8]$$

where $f(\tau)$ is a positive function normalized to one. As we show in *SI Appendix*, equations of this kind can be derived by coarse-graining spatial degrees of freedom in logistic or resource competition models (25). For example, if we consider a logistic equation with a diffusive term on a one-dimensional infinite chain, the dynamic equations after one step of spatial coarse graining are formally equivalent to Eq. **8**, with a tridiagonal delayed interaction

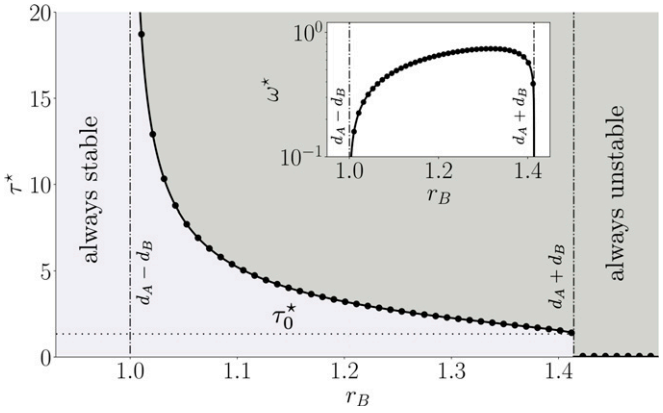

Fig. 2. Critical delay and critical frequency (*Inset*) curves as a function of $r_B = \sigma\sqrt{SC}$ for the system defined in Eq. **1**. The simulations (black dots) (*SI Appendix*) agree perfectly with the analytical prediction (black solid lines) given by Eqs. **5** and **6**. Here, we have considered $d_A = (\sqrt{2}+1)/2$ and $d_B = (\sqrt{2}-1)/2$. As $r_B \leq d_A - d_B$, the system is always stable, whereas it is always unstable when $r_B \geq d_A + d_B$. When $d_A - d_B < r_B < d_A + d_B$, the system changes its stability along the curve $\tau^\star(r_B)$. In addition, the presence of a finite jump ${\tau^\star}_0$ at $d_A + d_B$ as given by Eq. **7** shows that May's stability condition $r_B < d_A + d_B$ is still valid for $\tau < \tau_0^\star$.

matrix. This highlights the importance of the nonzero diagonal elements, at variance with what was studied in ref. 26. Also, when Eq. **8** is the result of a spatial coarse graining, in general the parameters d_A and d_B are no longer independent. A detailed derivation of this result is reported in *SI Appendix*.

As A and B commute, the equation for the eigenvalues reads

$$\lambda_i = a_i + b_i\,\mathcal{L}\,(\lambda_i), \qquad [9]$$

where $\mathcal{L}\,(\lambda) = \int_0^\infty f(\tau)e^{-\lambda\tau}\mathrm{d}\tau$ is the Laplace transform of $f(\tau)$. Under the same hypothesis that we have previously introduced, it is possible to derive a profile equation analogous to Eq. **4**, namely

$$d_B^2\mathcal{L}^I(\Lambda,\omega)^2 + \left[d_A + \Lambda + d_B\mathcal{L}^R(\Lambda,\omega)\right]^2 + \omega^2 + \\ + 2d_B\omega\mathcal{L}^I(\Lambda,\omega) = \left[\mathcal{L}^R(\Lambda,\omega)^2 + \mathcal{L}^I(\Lambda,\omega)^2\right] r_B^2. \quad [10]$$

Here, we indicate with $\mathcal{L}^R$ and $\mathcal{L}^I$ the real and imaginary parts of the Laplace transform. Clearly, if $f(\tau) = \delta\,(\tau - \tilde{\tau})$, Eq. **10** reduces to Eq. **4** (*SI Appendix*).

Let us consider the simple case of an exponential distribution $f(\tau) = e^{-\tau/\tilde{\tau}}/\tilde{\tau}$, where $\tilde{\tau}$ is the scale parameter. Now, Eq. **9** becomes a quadratic equation in λ (i.e., the eigenspectrum is formed by two branches). If we now substitute this expression in Eq. **10**, we get the curves reported in Fig. 3. The shape of the profile shrinks as the scale $\tilde{\tau}$ increases, and the system becomes more and more unstable as $\tilde{\tau}$ increases. However, if $\tilde{\tau}$ is large enough, the system eventually goes back to the stable regime, as shown in Fig. 3.

We now define two critical scale times $\tilde{\tau}^\star_-$ and $\tilde{\tau}^\star_+$, corresponding to the transitions from the stable to the unstable regime and vice versa. Two independent conditions at criticality can be obtained; for the case with exponentially distributed delay, if $d_A \geq d_B$, there is no solution, and the transition from the stable to the unstable regime occurs at $r_B^\star = d_A + d_B$. However, for $d_A < d_B$ and $2\sqrt{d_A\,d_B} < r_B < d_A + d_B$, the system admits two

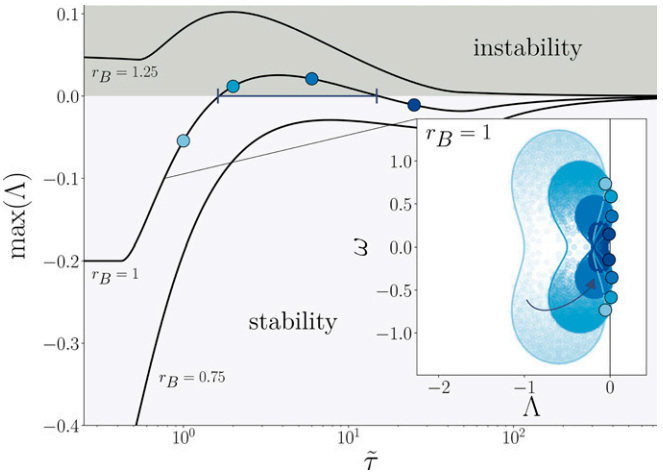

Fig. 3. Maximum of the real part Λ of the eigenspectrum of Eq. **8** for an exponentially distributed delay $f(\tau) = 1/\tilde{\tau}\,e^{-\tau/\tilde{\tau}}$ as a function of the temporal-scale parameter $\tilde{\tau}$. Here, $A = -d_A\mathbb{1}$ ($d_A = 0.2$), and B is a random matrix for three representative values of $r_B = \sigma\sqrt{CS}$ (black solid lines). When $r_B = 0.75$, the system is always stable since $\max\Lambda < 0$ for any $\tilde{\tau}$. Conversely, the system is always unstable for $r_B = 1.25$. When $r_B = 1$, as $\tilde{\tau}$ increases, the system is first stable; then, it transits to an instability region (as indicated by the horizontal segment), and finally, it goes back to the stability regime. This behavior is displayed in *Inset*, which shows the system eigenspectrum (color-coded circles) for some increasing values (according to the direction of the arrow) of $\tilde{\tau}$ when $r_B = 1$. The solutions of Eq. **10** (solid color-coded lines) and the points where the real part Λ of those curves is maximum (colored bordered circles) are reported for each $\tilde{\tau}$. Here, $d_A = 0.2$ and $d_B = 1$. In *Inset*, $C = 0.1$, $\sigma = 0.1$, and $S = 1{,}000$, so that $r_B = 1$, whereas $\tilde{\tau} = 1, 2, 6$, and 25.

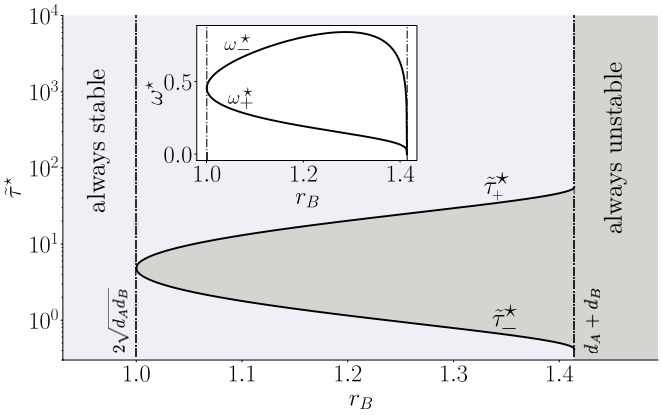

Fig. 4. Critical timescales $\tilde{\tau}^\star$ and the corresponding critical frequencies curves (*Inset*) given by Eqs. **11** and **12** as a function of $r_B = \sigma\sqrt{CS}$ for an exponentially distributed delayed system, as defined in Eq. **8**. An instability region is between the curves $\tilde{\tau}^\star{}_-$ and $\tilde{\tau}^\star{}_+$ (black solid lines). This means that when $2\sqrt{d_A d_B} < r_B < d_A + d_B$, the system is stable for small or large timescale $\tilde{\tau}$, while it is unstable for intermediate values. We have considered $d_A = \frac{\sqrt{2}-1}{2}$ and $d_B = \frac{\sqrt{2}+1}{2}$.

solutions $\tilde{\tau}^\star_-$ and $\tilde{\tau}^\star_+$ between which the system is unstable, with their corresponding $\omega^\star_-$ and $\omega^\star_+$. They are reported in Fig. 4 and read

$$\tilde{\tau}^\star{}_\pm = \frac{d_B - \chi \pm \sqrt{(d_B-\chi)^2 - d_A^2}}{d_A^2}, \qquad [11]$$

$$\omega^\star_\pm = d_A\sqrt{\chi\,\tilde{\tau}^\star{}_\pm}, \qquad [12]$$

with $\chi \equiv \sqrt{(d_A + d_B)^2 - r_B^2}$. For $r_B = 2\sqrt{d_A\,d_B}$, the two critical delays $\tilde{\tau}^\star_+$ and $\tilde{\tau}^\star_-$ coincide, whereas for larger values of r_B, they connect to the instability region.

Delay Effects on the Eigenspectrum Distribution

In addition to the geometric profile of the eigenspectrum, which rules the linear stability of the system, it is also possible to derive the complete eigenvalue distribution $\rho(\Lambda,\omega)$ as a function of the real and imaginary parts of λ. For the discrete delay case, in which A is diagonal and B is random, we obtain

$$\rho(\Lambda,\omega) = \frac{1}{\pi r_B^2}e^{2\Lambda\tau}\left[1 + 2\,(\Lambda + d_A)\,\tau \right. \\ \left. + \left(\omega^2 + (d_A+\Lambda)^2\right)\tau^2\right] \\ \times\,\mathcal{H}\left(r_B - \left|e^{\tau(\Lambda+i\omega)}(d_A + \Lambda + i\omega) + d_B\right|\right). \qquad [13]$$

The effect of the delay in this case is twofold, as illustrated in Fig. 5. On the one hand, the domain of the eigenspectrum defined by the Heaviside $\mathcal{H}(\cdot)$ function is no longer a circle, and it has multiple sectors as a consequence of the multiple branches of the Lambert $\mathcal{W}$ function in Eq. **3**. On the other hand, the presence of delay makes the distribution no longer uniform in its domain. In particular, the eigenvalues tend to accumulate to the rightmost part of each sector due to the exponential factor $e^{2\Lambda\tau}$ (Fig. 5).

For the case of an exponential distributed delay, the eigenspectrum distribution reads

$$\rho(\Lambda,\omega) = \frac{1}{\pi r_B^2}\mathcal{H}\left(r_B - |(\Lambda + i\omega + d_A)(1 + \Lambda + i\omega\tilde{\tau}) + d_B|\right) \\ \times\left[1 + 2\tilde{\tau}\,(d_A + 2\Lambda) + \left((d_A + 2\Lambda)^2 + (2\omega)^2\right)\tilde{\tau}^2\right], \qquad [14]$$

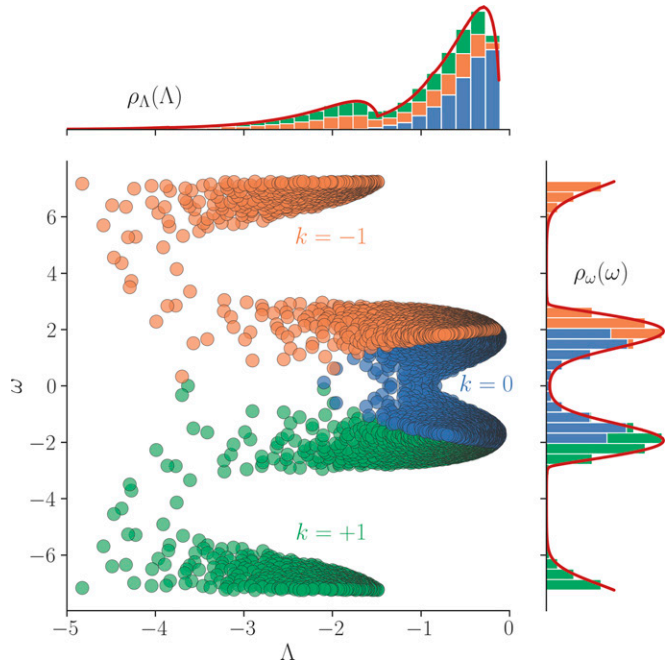

Fig. 5. Eigenvalues distribution for the system defined by Eq. **1** in the complex plane (Λ, ω). The principal branch ($k = 0$; in blue) is portrayed together with two other branches ($k = +1$ and $k = -1$; in green and orange, respectively) of the Lambert $\mathcal{W}$ function in Eq. **3**. The marginal distributions of Λ and the one of ω are represented in *Upper* and *Right*, respectively. They are in perfect agreement with the theoretical marginals $\rho_\Lambda(\Lambda)$ and $\rho_\omega(\omega)$ (solid red lines) obtained by integrating Eq. **13** in the intervals depicted. Here, $d_A = \frac{\sqrt{2}+1}{2}$, $d_B = \frac{\sqrt{2}-1}{2}$, $r_B = 1$, and $\tau = 1$.

which again breaks the circular law, although the absence of the exponential factor makes the distribution relatively more uniform with respect to Eq. **13**. These results can be easily adapted to other classes of random matrices B as long as the probability density function of their eigenspectrum is known. As an example, in *SI Appendix*, we have considered the class of symmetric random matrices whose eigenvalues are distributed according to Wigner's semicircle law. Although the eigenvalues of B are real, those of the system (1) are not always real. As soon as τ exceeds a critical threshold (which we calculate in *SI Appendix*), a complex branch emerges, where the real part is a function of the imaginary one. This line of eigenvalues may cross the imaginary axis for sufficiently large delays (*SI Appendix*, Fig. S5).

Discussion and Conclusions

In this work, we have applied random matrix theory and linear stability analysis to randomly assembled species governed by discrete- and distributed-time delay dynamics. Delay effects are indeed expected to be the rule rather than the exception in real systems and may originate from multiple sources; not all members of the same species are the same age, interacting partners are not necessarily affected simultaneously by their mutual interactions, and coarse graining of space may induce delayed self-interactions in mean field models.

We have first considered the effects of discrete delay, and we have found a generalization of May's bound. The critical delay curve does depend on the system size, thus generalizing the result in ref. 26 in which May's threshold was not changed. Delay may also induce oscillatory dynamics at the edge of instability (e.g., at the critical delay). We have determined the frequency delay curve of such oscillations as a function of the system size.

The previous equations with discrete or distributed delay dynamics assume that the amplitudes of the delayed interactions do not depend on the delay itself. This means that the effects of past populations densities on their current dynamics are independent of how far in the past they were generated. This is somehow unrealistic in real systems, where we expect that the amplitude of interactions is damped as the delay increases. This can be easily accommodated in the equations by replacing the matrix B with $f(\tau)B$, where $f(\tau)$ is a decreasing function of τ. In *SI Appendix*, we show that even a very slowly decreasing function extends the region of stability of an ecosystem.

In the case of an exponentially distributed delay, two critical curves emerge in the $r_b - \tilde{\tau}^*$ plane. These contain an instability region only for intermediate average delays, which was not present in the discrete case. We argue that such a feature is more general than the case considered here.

We have finally derived the full distributions of the eigenvalues that generalize Wigner's as well as Girko's laws. The presence of a temporal delay modifies not only the geometric profile of the eigenspectrum but also, the distribution of the eigenvalues. The generalized Wigner's law may have a line of complex eigenvalues that crosses the imaginary axis and destabilizes the system at high frequencies. The generalized Girko's law, instead, has marginal distributions, which are multimodal for both the real and imaginary parts of the eigenvalues. This is linked to the multiple branches of the Lambert $\mathcal{W}$ function, which is nonanalytic. The results obtained can also be adapted to other classes of interactions (e.g., mutualistic, antagonistic, predator–prey ones, etc.) as long as their eigenspectrum is known. We leave this characterization to future works.

We retrieve May's threshold when the random matrix B has zero diagonal entries, but our results lead to a generalization of May's stability condition that accounts for delayed self-interactions, which in general, play an important role in realistic situations. Of course, our approach should include further layers of complexity, such as environmental stochasticity (36) or more realistic species interactions, for modeling natural ecosystems. However, the proposed theoretical framework represents a first step toward the understanding of the delay effects in large ecosystems. Also, it can be a useful tool for studying the simple effects of delay on the stability of a wide range of different systems, including genetic networks (37, 38), brain dynamics (39), and financial systems (40).

Materials and Methods

Profile Equation for the Eigenvalues. When considering a discrete-time delay, the real and imaginary parts of Eq. **2** read

$$\Lambda = a + e^{-\tau\Lambda}\left(\mathrm{Re}\,[b]\cos\omega\tau + \mathrm{Im}\,[b]\sin\omega\tau\right), \qquad [15]$$

$$\omega = e^{-\tau\Lambda}\left(\mathrm{Im}\,[b]\cos\omega\tau - \mathrm{Re}\,[b]\sin\omega\tau\right), \qquad [16]$$

where we denote $\Lambda \equiv \mathrm{Re}[\lambda]$ and $\omega \equiv \mathrm{Im}[\lambda]$. This system gives Λ and ω in a parametric form, the parameters being the matrices eigenvalues [i.e., $a = -d_A$ and b, which belongs to the circle centered at $(-d_B; 0)$ with radius $r_B = \sigma\sqrt{SC}$]. Therefore, since the equation for λ is analytic in $\mathbb{C}$, it is possible to describe (part of) the profile of λ by fixing b on the circumference (i.e., by setting $\mathrm{Re}\,[b] = -d_B + r_B\cos\theta$ and $\mathrm{Im}\,[b] = r_B\sin\theta$). The profile Eq. **4** of the eigenvalues λ is then obtained by noting that Eqs. **15** and **16** must satisfy the identity $\cos^2\theta + \sin^2\theta = 1$.

On the other hand, when studying a distributed delay, the real and imaginary parts of Eq. **9** are

$$\Lambda = -d_A + \mathrm{Re}(b)\mathcal{L}^R(\Lambda,\omega) - \mathrm{Im}(b)\mathcal{L}^I(\Lambda,\omega), \qquad [17]$$

$$\omega = \mathrm{Im}(b)\mathcal{L}^R(\Lambda,\omega) + \mathrm{Re}(b)\mathcal{L}^I(\Lambda,\omega), \qquad [18]$$

where we remind that $\mathcal{L}^R$ and $\mathcal{L}^I$ are the real and imaginary parts of the uniform Laplace transform. Eq. **10** follows analogously.

Critical Delay and Frequency. Let us consider the profile equation for the discrete delayed system given by Eq. **4**. From this equation, it is possible to obtain two independent conditions for determining $\tau^\star$ and the corresponding critical frequency $\omega^\star$, at which the transition from the stable to the unstable regime occurs. In particular, the first requirement is simply that $\Lambda = 0$ when $\tau = \tau^\star$. Hence,

$$d_B^2 + d_A^2 + \omega^{\star 2} + 2d_B \left[d_A \cos\left(\omega^\star \tau^\star\right) - \omega^\star \sin\left(\omega^\star \tau^\star\right)\right] = r_B^2. \quad [19]$$

A second condition can be obtained by parameterizing the profile curve as $\Lambda = \Lambda(\omega)$ and constraining $\Lambda(\omega)$ to have a maximum at $\tau = \tau^\star$. From this, we get the following equation:

$$\left(1 + d_A \tau^\star\right) d_B \sin\left(\omega^\star \tau^\star\right) + d_B \omega^\star \tau^\star \cos\left(\omega^\star \tau^\star\right) = \omega^\star. \quad [20]$$

Eqs. **19** and **20**, thus, give the conditions that define $\tau^\star$ and $\omega^\star$. The analogous derivation for a distributed delay is reported in *SI Appendix*. In the particular case of an exponential distribution, the two conditions read

$$\frac{\left(d_A + d_B\right)^2 - r_B^2 + \omega^{\star 2}}{\left(\omega^\star \tilde{\tau}^\star\right)^2} = \frac{2d_B}{\tilde{\tau}^\star} - \left(d_A^2 + \omega^{\star 2}\right), \quad [21]$$

$$\frac{\omega^\star}{\tilde{\tau}^\star}\left[\tilde{\tau}^{\star 2}\left(d_A^2 + 2\omega^{\star 2}\right) - 2d_B\tilde{\tau}^\star + 1\right] = 0, \quad [22]$$

whose solutions are given by Eqs. **11** and **12**.

Eigenvalues Distribution. Let $A = -d_A \mathbb{1}$ and B be a random matrix whose eigenvalues follow a distribution $p(b)$, which for the particular class considered throughout this work, is the uniform distribution given by the circle law: that is,

$$p(b) = \frac{1}{\pi r_B^2} \mathcal{H}\left(r_B - |b + d_B|\right). \quad [23]$$

To our purpose, it is convenient to consider $p(b)$ as a function of two real variables (i.e., the real and imaginary parts of b) rather than a function of a complex variable. Indeed, if we know such probability distribution, we can exploit it to get

$$\rho(\Lambda, \omega) = p(b(\Lambda, \omega)) \left|\det J_{b(\Lambda,\omega)}\right|, \quad [24]$$

where again, $b(\Lambda, \omega)$ is a vector whose components are the real and imaginary parts of the inverse transformation of $\lambda(b)$ and $J_{b(\Lambda,\omega)}$ is the Jacobian of this transformation. For a discrete delay, $\lambda(b)$ is given by Eq. **2**, and the two components of $b(\Lambda, \omega)$ read

$$\mathrm{Re}\left[b(\Lambda, \omega)\right] = e^{-\Lambda\tau}\left[\left(d_A + \Lambda\right)\cos\omega\tau + \omega \sin\omega\tau\right], \quad [25]$$

$$\mathrm{Im}\left[b(\Lambda, \omega)\right] = e^{-\Lambda\tau}\left[\omega\cos\omega\tau - \left(d_A + \Lambda\right)\sin\omega\tau\right]. \quad [26]$$

Therefore, the determinant of the Jacobian is

$$\left|\det J_{b(\Lambda,\omega)}\right| = e^{2\Lambda\tau}\left[1 + 2\left(\Lambda + d_A\right)\tau + \left(\omega^2 + \left(d_A + \Lambda\right)^2\right)\tau^2\right], \quad [27]$$

and Eq. **13** follows immediately. A parallel derivation also can be done for the distributed delay, starting from Eq. **9** (*SI Appendix*), which for the exponential distribution, leads to Eq. **14**.

Data, Materials, and Software Availability. Python code for numerical simulations has been deposited in GitHub (https://github.com/epigani/DelayEffects) (41).

ACKNOWLEDGMENTS. E.P. acknowledges D. M. Busiello for insightful discussions and valuable suggestions. E.P. acknowledges a fellowship funded by the Stazione Zoologica Anton Dohrn (SZN) within the SZN Open University PhD program. E.P. and A.M. are supported by "Excellence Project 2018" funded by the Cariparo Foundation. S.S., A.M, and S.A. also acknowledge Istituto Nazionale di Fisica Nucleare (INFN) for a Lincoln grant and a Budget Integrato della Ricerca di Dipartimento, Dipartimento di Fisica e Astronomia, Università degli Studi di Padova (UNIPD DFA BIRD2021) grant.

1. P. W. Anderson, More is different. *Science* **177**, 393–396 (1972).
2. T. M. Liggett, T. M. Liggett, *Interacting Particle Systems* (Springer, 1985), vol. 2.
3. J. H. Holland, Complex adaptive systems. *Daedalus* **121**, 17–30 (1992).
4. L. N. Amaral, S. V. Buldyrev, S. Havlin, M. A. Salinger, H. E. Stanley, Power law scaling for a system of interacting units with complex internal structure. *Phys. Rev. Lett.* **80**, 1385 (1998).
5. F. Peruzzo, M. Mobilia, S. Azaele, Spatial patterns emerging from a stochastic process near criticality. *Phys. Rev. X* **10**, 011032 (2020).
6. J. Gao, B. Barzel, A. L. Barabási, Universal resilience patterns in complex networks. *Nature* **530**, 307–312 (2016).
7. C. Tu, J. Grilli, F. Schuessler, S. Suweis, Collapse of resilience patterns in generalized Lotka-Volterra dynamics and beyond. *Phys. Rev. E* **95**, 062307 (2017).
8. S. Butler, J. P. O'Dwyer, Stability criteria for complex microbial communities. *Nat. Commun.* **9**, 2970 (2018).
9. C. Tu, S. Suweis, J. Grilli, M. Formentin, A. Maritan, Reconciling cooperation, biodiversity and stability in complex ecological communities. *Sci. Rep.* **9**, 5580 (2019).
10. S. Allesina, S. Tang, Stability criteria for complex ecosystems. *Nature* **483**, 205–208 (2012).
11. S. Allesina, S. Tang, The stability–complexity relationship at age 40: A random matrix perspective. *Popul. Ecol.* **57**, 63–75 (2015).
12. R. M. May, Will a large complex system be stable? *Nature* **238**, 413–414 (1972).
13. T. Galla, Random replicators with asymmetric couplings. *J. Phys. Math. Gen.* **39**, 3853 (2006).
14. M. Barbier, J. F. Arnoldi, G. Bunin, M. Loreau, Generic assembly patterns in complex ecological communities. *Proc. Natl. Acad. Sci. U.S.A.* **115**, 2156–2161 (2018).
15. C. A. Serván, J. A. Capitán, J. Grilli, K. E. Morrison, S. Allesina, Coexistence of many species in random ecosystems. *Nat. Ecol. Evol.* **2**, 1237–1242 (2018).
16. Y. Krumbeck, Q. Yang, G. W. A. Constable, T. Rogers, Fluctuation spectra of large random dynamical systems reveal hidden structure in ecological networks. *Nat. Commun.* **12**, 3625 (2021).
17. J. Hofbauer *et al.*, *Evolutionary Games and Population Dynamics* (Cambridge University Press, 1998).
18. M. Saeedian, E. Pigani, A. Maritan, S. Suweis, S. Azaele, Effect of delay on the emergent stability patterns in generalized Lotka-Volterra ecological dynamics. *Philos. Trans.- Royal Soc., Math. Phys. Eng. Sci.* **380**, 20210245 (2022).
19. Y. V. Fyodorov, B. A. Khoruzhenko, Nonlinear analogue of the May-Wigner instability transition. *Proc. Natl. Acad. Sci. U.S.A.* **113**, 6827–6832 (2016).
20. G. Ben Arous, Y. V. Fyodorov, B. A. Khoruzhenko, Counting equilibria of large complex systems by instability index. *Proc. Natl. Acad. Sci. U.S.A.* **118**, e2023719118 (2021).
21. G. Biroli, G. Bunin, C. Cammarota, Marginally stable equilibria in critical ecosystems. *New J. Phys.* **20**, 083051 (2018).
22. A. Altieri, F. Roy, C. Cammarota, G. Biroli, Properties of equilibria and glassy phases of the random Lotka-Volterra model with demographic noise. *Phys. Rev. Lett.* **126**, 258301 (2021).
23. M. T. Pearce, A. Agarwala, D. S. Fisher, Stabilization of extensive fine-scale diversity by ecologically driven spatiotemporal chaos. *Proc. Natl. Acad. Sci. U.S.A.* **117**, 14572–14583 (2020).
24. F. Roy, M. Barbier, G. Biroli, G. Bunin, Complex interactions can create persistent fluctuations in high-diversity ecosystems. *PLoS Comput. Biol.* **16**, e1007827 (2020).
25. D. Gupta, S. Garlaschi, S. Suweis, S. Azaele, A. Maritan, Effective resource competition model for species coexistence. *Phys. Rev. Lett.* **127**, 208101 (2021).
26. V. K. Jirsa, M. Ding, Will a large complex system with time delays be stable? *Phys. Rev. Lett.* **93**, 070602 (2004).
27. E. Niebur, H. G. Schuster, D. M. Kammen, Collective frequencies and metastability in networks of limit-cycle oscillators with time delay. *Phys. Rev. Lett.* **67**, 2753–2756 (1991).
28. T. Ohira, Y. Sato, Resonance with noise and delay. *Phys. Rev. Lett.* **82**, 2811 (1999).
29. J. E. Forde, *Delay Differential Equation Models in Mathematical Biology* (University of Michigan, 2005).
30. J. D. Murray, *Mathematical Biology I. An Introduction* (Springer, 2002).
31. Y. Kuang, *Delay Differential Equations* (University of California Press, 2012).
32. J. E. Cohen, C. M. Newman, The stability of large random matrices and their products. *Ann. Probab.* **12**, 283–310 (1984).
33. H. L. Smith, *An Introduction to Delay Differential Equations with Applications to the Life Sciences* (Springer, New York, NY, 2011), vol. 57.
34. S. Ruan, On nonlinear dynamics of predator-prey models with discrete delay. *Math. Model. Nat. Phenom.* **4**, 140–188 (2009).
35. R. M. Corless, G. H. Gonnet, D. E. Hare, D. J. Jeffrey, D. E. Knuth, On the lambertw function. *Adv. Comput. Math.* **5**, 329–359 (1996).
36. R. Rebolledo, S. A. Navarrete, S. Kéfi, S. Rojas, P. A. Marquet, An open-system approach to complex biological networks. *SIAM J. Appl. Math.* **79**, 619–640 (2019).
37. K. Josić, J. M. López, W. Ott, L. Shiau, M. R. Bennett, Stochastic delay accelerates signaling in gene networks. *PLoS Comput. Biol.* **7**, e1002264 (2011).
38. C. Gupta, J. M. López, W. Ott, K. Josić, M. R. Bennett, Transcriptional delay stabilizes bistable gene networks. *Phys. Rev. Lett.* **111**, 058104 (2013).
39. G. Stepan, Delay effects in brain dynamics. Introduction. *Philos. Trans. A Math. Phys. Eng. Sci.* **367**, 1059–1062 (2009).
40. W. C. Chen, Dynamics and control of a financial system with time-delayed feedbacks. *Chaos Solitons Fractals* **37**, 1198–1207 (2008).
41. E. Pigani, Code for "Delay effects on the stability of large ecosystems." GitHub. https://github.com/epigani/DelayEffects. Deposited 4 July 2022.